

Induced geoelectric field calculations during magnetic storms in the Balearic Islands

Author: Nora Bonmatí Oviedo

Facultat de Física, Universitat de Barcelona, Diagonal 645, 08028 Barcelona, Spain.

Advisor: Dra. Anna Martí Castells

Abstract: This study aims to analyze the surface induced electric fields resulting from 11 solar storms to create a potential risk map for future electrical infrastructures. The research employed a 3D electrical resistivity model of the Balearic Islands and a program based on spherical elementary current systems for magnetic field interpolation, due to the lack of observatories, correlating electric and magnetic fields using the magnetotelluric method. The study involved generating electric field maps and exploring the relationship between the electric field magnitude over the islands and solar activity. Outcomes revealed cases of abrupt electric field intensities for solar activity in certain locations across the Balearic Islands resulting in risks to electrical grids.

I. INTRODUCTION

Space weather is a branch of space physics that, among other phenomena, studies the interaction between the Solar wind particles and the Earth's magnetic field. Geomagnetic storms occur when the flow of these particles is anomalously high, capable of causing large fluctuations in the Earth's magnetic field and potentially inducing significant geoelectric fields at the Earth's surface. These geoelectric fields can generate induced currents (Geomagnetically Induced Currents or GICs), which are a function of the geoelectric fields and the network parameters. They may flow through the power network with the potential to damage its components, even at mid and low latitudes. For instance, the Halloween storm (29/10/2003) had important magnetic field variations in $25^{\circ}S$ and $35^{\circ}S$ geomagnetic latitudes and caused significant GICs [1].

In order to design and build resilient electrical infrastructures, it is important to have a clear picture of the geoelectric fields that can be potentially generated by geomagnetic storms in a specific territory, in order to map the areas that are more vulnerable if power network elements are present. The geoelectric fields are dependant upon the intensity and direction of the geomagnetic field, which also depends on the latitude, and on the electrical resistivity of the Earth, particularly the lithosphere [1].

To characterize the resistivity of the lithosphere, we work with the magnetotelluric exploration method. The MT allows the determination of resistivity distribution in the subsurface by measuring the time variations of both electric and magnetic fields. The relationship between their horizontal components in the frequency domain is the impedance tensor ($Z(\omega)$). Therefore, by having a resistivity model and knowing the magnetic field on the surface, we can determine the electric field. In this study, we will focus on the calculation and analysis of the electric fields generated by magnetic storms. There is already a 3D resistivity model of the Balearic island [1] based on geological and geophysical information [4] and with the impedance tensors calculated in the Mallorca island with MT.

Once this information is known, the magnetic empir-

ical data is acquired from diverse observatories. In this scenario, the Balearic Islands do not have any geomagnetic observatories. Hence, we employed a modeling approach to estimate geoelectric fields using observatories located near, but not within, the Balearic Islands. J. Campanyà's program [3] employs a spherical elementary current system to interpolate magnetic fluctuations between geomagnetic observatories and the location of interest utilizing the measured MT impedance tensor.

Geoelectric fields and GICs have already been calculated for locations within the existing power network in the Balearic Archipelago [1]. This investigation aims to calculate the electric field on the surface based on the subsurface resistivity model, utilizing data from 11 solar storms and five different observatories in order to create a risk map for a potential electrical grid.

II. MAGNETOTELLURIC GEOPHYSICAL EXPLORATION

The magnetotelluric method is an electromagnetic geophysical exploration technique employed to characterize the Earth subsurface structures by analyzing its electrical resistivity distribution. It relies on the natural electromagnetic field as its energy source. The MT exploration provides us with a multitude of possibilities, such as the ability to explore at significant depths. Exploration depth depends on the signal's frequency, and there is a wide range, from tenths of meters to hundreds of kilometers [5].

Experimentally, it involves four electrodes positioned in the north-south and east-west directions, capable of measuring both the E_x and E_y components of the electric field. The potential difference between the pair of electrodes, which are set apart by a specific distance, is calculated to determine the electric field. Furthermore, for the calculation of the magnetic field, induction coils or fluxgate magnetometer are employed.

The physics governing MT is described by Maxwell's equations.

$$\begin{aligned}
 \vec{\nabla} \cdot \vec{D} &= \rho_V && \text{Gauss's Law for Electricity} \\
 \vec{\nabla} \cdot \vec{B} &= 0 && \text{Gauss's Law for Magnetism} \\
 \vec{\nabla} \times \vec{E} &= -\frac{\partial \vec{B}}{\partial t} && \text{Faraday's Law} \\
 \vec{\nabla} \times \vec{H} &= \vec{j} + \frac{\partial \vec{D}}{\partial t} && \text{Ampère's Law,}
 \end{aligned} \tag{1}$$

Where \vec{D} is the electric displacement, ρ_V the electric charge density, \vec{E} and \vec{H} are the electric and magnetic fields, \vec{B} is the magnetic induction and \vec{j} and $\frac{\partial \vec{D}}{\partial t}$ are the current density and the displacement current.

However, MT operates within the frequency domain so we have to Fourier Transform. In this domain, the Faraday and Ampère's laws can be expressed as follows:

$$\begin{aligned}
 \vec{\nabla} \times \vec{E} &= -i\omega \vec{B} \\
 \vec{\nabla} \times \vec{H} &= \mu\sigma \vec{E},
 \end{aligned} \tag{2}$$

Where ω represents the angular frequency of the electromagnetic oscillations and μ the magnetic permeability.

Now, we introduce the impedance tensor, which establishes a relationship between the magnetic and electric horizontal components at a specific frequency.

$$\begin{pmatrix} E_x(\omega) \\ E_y(\omega) \end{pmatrix} = \begin{pmatrix} M_{xx} & M_{xy} \\ M_{yx} & M_{yy} \end{pmatrix} \begin{pmatrix} B_x(\omega) \\ B_y(\omega) \end{pmatrix} \tag{3}$$

We can express $M_{ij} = |M_{ij}|e^{i\phi}$ in the polar form. At this point, we can define two real magnitudes:

$$\begin{aligned}
 \rho_{ij}(\omega) &= \frac{\mu_0}{\omega} |M_{ij}|^2 \\
 \phi_{ij}(\omega) &= \text{arctg} \left(\frac{\text{Im}(M_{ij}(\omega))}{\text{Re}(M_{ij}(\omega))} \right)
 \end{aligned} \tag{4}$$

ρ_{ij} represents the apparent resistivity, which is the average resistivity along the path of electromagnetic wave travel, while ϕ_{ij} is the impedance phase. The impedance phase is sensitive to changes in the apparent resistivity and remains unaffected, for instance, by galvanic effects that certainly impact the apparent resistivity.

III. BALEARIC GEOELECTRICAL MODEL

The Balearic Islands are located in the Western Mediterranean, in the Eastern coast of the Iberian Peninsula. They are the NE continuation of the Betic chain, raised on the Balearic Promontory platform, located SW of the Valencia Trough extensional basin. A 3D electrical resistivity model of the Balearic Islands was built through geological and geophysical information [4]. The properties of the crustal and lithospheric structure data

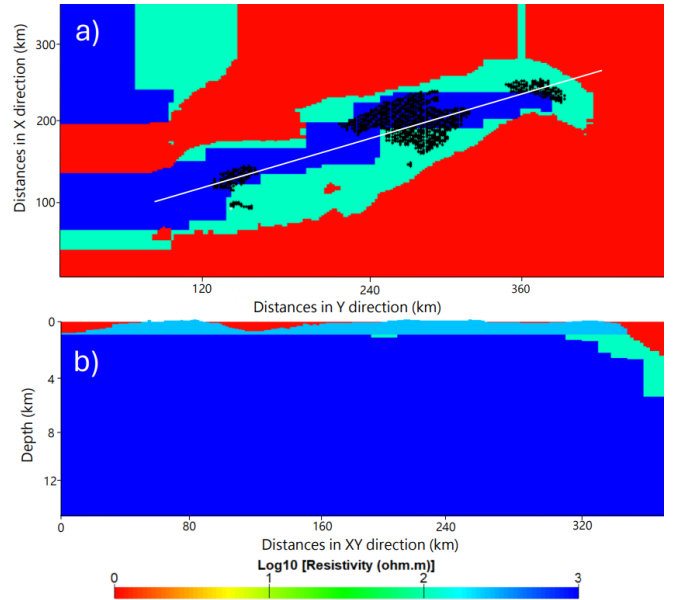


FIG. 1: Resistivity model of the Balearic Archipelago. (a) Horizontal cross section of the electrical resistivity model at a depth of 0.95 km beneath sea level. (b) Cross-section of the XY plane represented with a white line in Figure 1.a, with a depth of 15 km..

were obtained through various methods, including the analysis of seismic data and the study of the geodynamic evolution of the Valencia Trough.

We must know that the Earth composition have a wide range of resistivities. As observed in the model (Figure 1), water containing dissolved ions demonstrates higher conductivity, with its resistivity approximately in the range of a few tenths. Yet, the sediments within the lithosphere have a lower conductivity ($\sim 100 \Omega \cdot m$), although not as much as that of the crust ($\sim 1500 \Omega \cdot m$). However, the mobility of charged particles in the asthenosphere is greater. Consequently, it has higher conductivity ($\sim 50 \Omega \cdot m$).

The model responses were calculated at the surface, at measuring points called sites, forming a grid with 1.016 sites distributed along the five islands, each having an area of $2 \times 2 \text{ km}^2$. These sites will serve as the locations for obtaining simulated data on the electric field.

Electromagnetic fields, both natural and artificial, interact with these materials in specific ways, which is precisely what magnetotelluric exploration utilizes to characterize Earth's subsurface. Having already a resistivity model, it allows the calculation of the electric field at the surface induced by a magnetic field. In this study, the magnetic field under consideration are solar storms.

IV. DATA PROCESSING

For data processing, a program [3] has been used to obtain the value of the magnetic field on the surface without

the need for a physical observatory in the exploration area. Data obtained from close magnetic observatories was employed to interpolate and derive the magnetic field for each site, using Spherical Elementary Current System. The SECS is a method used in geophysics to model the magnetic field changes on the Earth's surface. It is based on the idea that these variations can be described by a set of currents in the ionosphere. These currents are considered to be divergence-free as their behavior in actual conditions [3].

The observatories used for this study were Ebro (EBR), San Pablo-Toledo (SPT), San Fernando (SFS), Chambon-la-Foret (CLF) and L'Aquila (AQU), that are part of the INTERMAGNET network. They are all represented in Figure 2.

The data of the magnetic field variation used were characterized by a sampling rate of 1 minute and periods of 1 day. Days with strong solar activity were chosen based on the Kp and Ap index. The Kp index is a value used to quantify the disturbances of the geomagnetic field caused by a solar storm. It ranges from 0 to 9, based on the observations of the horizontal component of the magnetic field from 13 selected observatories, providing information on a global-scale. The Ap index follows a similar concept, but it utilizes a linear scale instead of a semilogarithmic one [6].

A total of 11 geomagnetic storms were chosen based on a minimum value of $Kp = 5+$, approximately equivalent to $Ap = 56$.

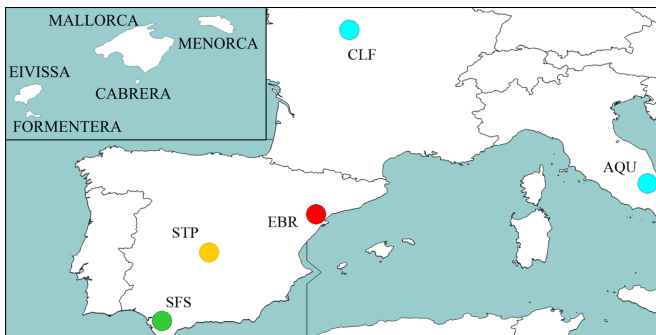


FIG. 2: Location of the observatories used for the study of the magnetic field. Are represented in red, the observatories within a distance of less than 200 km from the islands; in yellow, those within 500 km; in green, within 1000 km; and in blue, within 1200 km. In the box, the five islands are represented with their respective names.

Additionally, it should be noted that some extra maps of the geoelectric field were created using not all of the observatories listed in Table I, to verify that the number and arrangement of observatories did not significantly alter the results of the electric field calculation. Differences could be observed, but these did not deviate significantly from the results obtained taking into account all observatories.

TABLE I: Table showing the dates of the studied solar storms, their Ap index value, the maximum modulus of the geoelectric field on the islands (mV/km), and the observatories used for the interpolation.

Date	Ap	$ E _{\max}$ (mV/km)	Observatories
06/04/2000	56	322	CLF, EBR, SPT
15/07/2000	180	779	AQU, CLF, EBR, SPT
12/08/2000	109	144	AQU, CLF, EBR, SPT
06/11/2001	112	566	AQU, CLF, EBR, SPT
29/10/2003	240	1346	AQU, CLF, EBR, SPT
20/11/2003	115	674	AQU, CLF, EBR, SPT
27/07/2004	162	143	AQU, CLF, EBR, SPT
08/11/2004	189	419	AQU, CLF, EBR, SPT
15/05/2005	105	651	AQU, CLF, EBR, SFS, SPT
24/08/2005	110	658	AQU, CLF, EBR, SFS, SPT
17/03/2015	117	349	CLF, EBR, SFS, SPT

V. RESULTS

I have analyzed the trend and intensity of the surface electric and magnetic fields for the solar storms listed in Table I, although only two of them have been plotted. In Figures 3 and 4, vectors have not been depicted for all sites to provide a clearer overview of the electric field directions.

Despite variations in the distribution of the magnetic field among different solar storms, it exists a similarity in both magnitude and direction of the electric field across all storms.

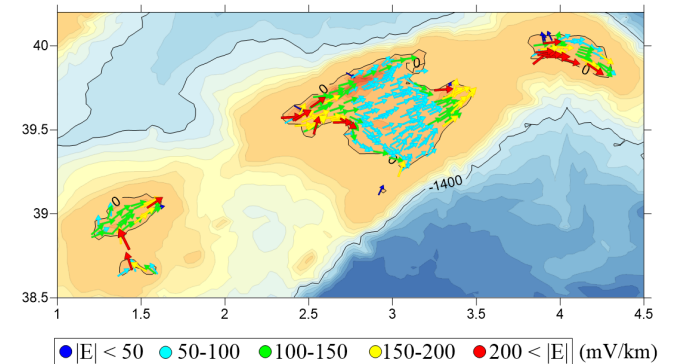


FIG. 3: Map of the Balearic archipelago where the maximum value of the geoelectric field is represented during the St. Patrick's Day solar storm (17/03/2015). The color scheme corresponds to the intensity of the surface electric field value.

Figures 3 and 4 demonstrate a general tendency for the geoelectric field to follow the path of the Balearic Promontory platform. Moreover, it also appears that the electric field pointed towards the nearest islands. In Cabrera and Formentera, the electric field lines extend towards the shores of their closest islands. Conversely, those from Mallorca and Eivissa stretch toward Cabrera

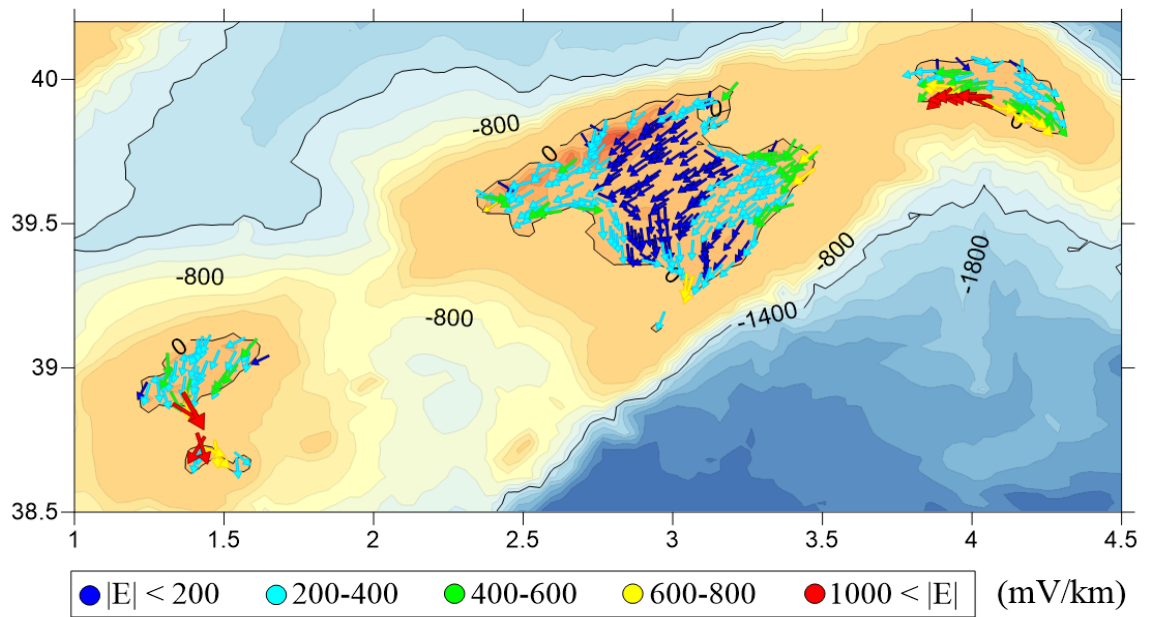


FIG. 4: Map of the Balearic archipelago where the maximum value of the geoelectric field is represented during the Halloween solar storm (29/10/2003). The color scheme corresponds to the intensity of the surface electric field value.

and Formentera.

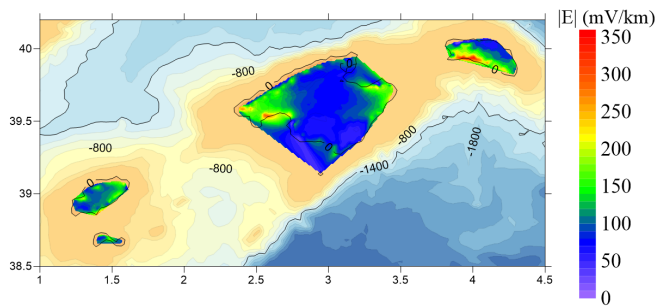


FIG. 5: Map depicting the maximum intensity of the electric field on the surface of the Balearic Archipelago during the St. Patrick's Day solar storm (17/03/2015).

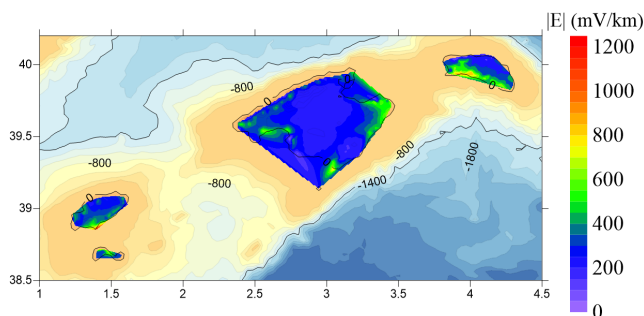


FIG. 6: Map depicting the maximum intensity of the electric field on the surface of the Balearic Archipelago during the Halloween solar storm (29/10/2003).

Additionally, as seen in Figures 5 and 6, an accumulation of large electric fields can be observed in the same places for any given solar storm. These spots coincide mostly with high resistivity locations as we can see in Figure 1. The center of Mallorca seems to not be very affected by an increase of solar activity as it is the north of Menorca and Eivissa. The electric field appears to be more intense at the edges of Mallorca, specifically the northwest and southeast edges of the island. In terms of resistivity, as depicted in Figure 1, these areas of the island are modeled with slightly the same resistivity. The reason for the notable change in the magnitude of the electric field in these areas could be related to the type of material and arrangement in the subsurface. It could also be due to the interaction that the islands might provoke among themselves. In the case of Mallorca, the two ends with a higher magnitude of the electric field are the closest parts to the adjacent islands. This behavior could also be observed to a lesser extent between Cabrera and Mallorca.

Given that Eivissa appears to be significantly affected by intense solar activity, in Figure 7 the modulus of its geoelectric field has been represented as a function of the *Ap index* to evaluate any potential correlation and determine if these areas present a risk.

There is an observable growth pattern in the electric field's modulus as the *Ap index* increases. This phenomenon is evidenced by the correlation coefficient between the geoelectrical modulus and the *Ap index*. Due to the fact that only 11 solar storms were studied, the result of a correlation is not that clear.

Furthermore, it is also observed that Eivissa tends to experience a fast growth, leading to high electrical field

intensities in certain areas, especially in the southern part of the island. The nonlinearity may also be due to the complexity of the geoelectric structure.

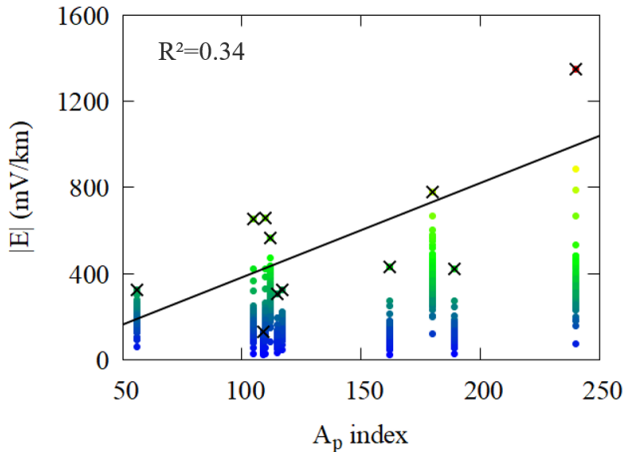


FIG. 7: Scatter plots of electrical field modulus (mV/km) time series for all site locations in Eivissa, as a function of the A_p index for all 11 solar storms. The (\times) symbol represents the largest electrical modulus, while the regression line fits these values.

In the study of Eivissa, if we exclude the solar storm of (08/11/2004), we observe an increase from an $R^2 = 0.34$ to $R^2 = 0.61$. This demonstrates the need for further study of more solar storms to determine the real trend and correlation. Nonetheless, this initial study serves as a first step to observe, on a large scale, the peculiar behavior of the electric field arrangement.

VI. CONCLUSIONS

We have studied the response of the electric field to various solar storms through measurements from multiple observatories. Despite examining different storms, we have identified patterns in the behavior of the electric

field and estimated a correlation between its variation and the storm's intensity. In some locations, the storm intensity followed a proportionality with the generated electric field. Although the nonlinearity could be due to the complexity of the subsurface.

It has been proven that neither the arrangement nor the number of observatories used could have modified the final geoelectric field result, eliminating any doubt that this factor could lead us away from reality.

It has been observed that placing electrical infrastructure, such as transformers, in the southern areas of Eivissa and Menorca could be hazardous, as these regions typically exhibit the most intense electric fields among the islands. Large electric fields were also observed in the south of the island of Formentera and at the two north-western and south-eastern ends of the island of Mallorca. This largely corresponded to areas of higher resistivity, but it may not be the only explanation. A peculiar behavior has been observed at the ends of the islands closest to each other. They could be interacting among themselves and causing unknown effects, leading to high intensities in these areas. Unlikely, there are many parameters to consider in order to parameterize the response of the electric field, not only the resistivity of the isolated island but also the overall layout. Nevertheless, as it is a model, it does not represent reality in detail but captures the most characteristic features.

This work reinforces the idea that a more detailed study can be conducted by examining additional storms to validate the obtained results.

Acknowledgments

I would like to thank Anna Martí, for her guidance and support throughout this study. Working with her has been a pleasure and I have learned a lot about this area of physics. Finally, I want to express my sincere thanks to my family and friends for their support during my degree.

-
- [1] Torta, J. M., Marsal, S., Piña-Varas, P., Hafizi, R., Martí, A., Campanyà, J., et al. (2023). Expected geomagnetically induced currents in the Spanish islands power transmission grids. *Space Weather*, 21, e2023SW003426. <https://doi.org/10.1029/2023SW003426>
- [2] Torta, J. M., Marsal, S., Ledo, J., Queralt, P., Canillas-Pérez, V., Piña-Varas, P., et al. (2021). New detailed modeling of GICs in the Spanish power transmission grid. *Space Weather*, 19, e2021SW002805. <https://doi.org/10.1029/2021SW002805>
- [3] Campanyà, J., Gallagher, P. T., Blake, S. P., Gibbs, M., Jackson, D., Beggan, C. D. et al. (2019). Modeling geoelectric fields in Ireland and the UK for space weather applications. *Space Weather*, 17, 216–237. <https://doi.org/10.1029/2018SW001999>
- [4] Ayala, C., Torne, M. and Roca, E., (2015). A review of the current knowledge of the crustal and lithospheric structure of the Valencia Trough Basin. *Boletín Geológico y Minero*, 126, 533-552.
- [5] Martí, A., (2006). A magnetotelluric investigation of geoelectric dimensionality and study of the Central Betic crustal structure. PhD Dissertation, Universitat de Barcelona, 306 pp. <http://www.tdx.cat/TDX-0115107-115853S>
- [6] Marshall, R., Dziura, L., Wang, L., Young, J., & Terkildsen, M. (2020). Estimating extreme geoelectric field values for the Australian region. *Space Weather*, 18, e2020SW002512. <https://doi.org/10.1029/2020SW002512>